Runup and uncertainty quantification: sensitivity analysis via ANOVA decomposition

Mario Ricchiuto, Pietro Marco Congedo, Argiris I. Delis

Runup and uncertainty quantification: sensitivity analysis via ANOVA decomposition

Mario Ricchiuto, Pietro Marco Congedo and Argiris Delis

RESEARCH REPORT

N° 8530

April 2014

Project-Team BACCHUS

ISSN 0249-6399

Runup and uncertainty quantification: sensitivity analysis via ANOVA decomposition

M. Ricchiuto[1], P.M. Congedo[2],
A.I. Delis[3]
Project-Teams BACCHUS

Research Report N° 8530 — 01/04/2014 —15 pages.

Abstract: We investigate the ability of uncertainty quantification techniques to act as enablers for the study of the sensitivity of dynamics of dam breaks to the variations of model parameters. In particular, we make use of sensitivity indexes computed by means of an Analysis of Variance (ANOVA) to provide the sensitivity of the runup dynamics to the variations of parameters such wave amplitude, friction coefficient, etc. The sensitivity indexes, known as Sobol indexes, are obtained following (Crestaux-LeMaitre-Martinez, 2009) by resorting to a non-intrusive polynomial chaos method allowing to reconstruct a complete representation of the variation of the outputs in the parameter space, and to compute the sensitivity indexes via the ANOVA decomposition. To increase the reliability of the results, we perfom the study independently with two models based on a discretization of the shallow water equations, developed in (Ricchiuto, 2014), and (Nikolos and Delis, 2009), respectively. The approach proposed provides simultaneously the variance of the outputs and their sensitivity to each independent parameter, allowing to construct a hierarchy of parameters which depends on the flow conditions.

Key-words: Runup, uncertainty propagation, analysis of variance, amplitude, friction, slope, parameter sensitivity

[1] Inria Bordeaux Sud-Ouest, BACCHUS Team – mario.ricchiuto@inria.fr

[2] Inria Bordeaux Sud-Ouest, BACCHUS Team – pietro.congedo@inria.fr

[3] Technical University of Crete – adelis@science.tuc.gr

RESEARCH CENTRE
BORDEAUX - SUD-OUEST

351 Cours de la Libération
Bâtiment A29
33405 Talence Cedex France

Runup and uncertainty quantification: sensitivity analysis via ANOVA decomposition

Résumé : Nous étudions l'utilisation de techniques incertitude de quantification pour l'étude de la sensibilité de la dynamique du runup variations de paramètres du modèle utilisé. En particulier, nous basons l'étude de sensibilité sur des indices calculés au moyen d'une analyse de variance (ANOVA) pour fournir la sensibilité de la dynamique de l'inondation aux variations de paramètres tels que l'amplitude de l'onde, le coefficient de frottement, etc. Les indices de sensibilité, appelés indices de Sobol, sont obtenus en recourant à une technique de type chaos polynômiale non-intrusif (Crestaux - Lemaître- Martinez , 2009) utilisée à la fois pour reconstruire une représentation complète de la variation des sorties dans l'espace des paramètres, et aussi pour calculer les indices de sensibilité par la décomposition de variance. Pour augmenter la fiabilité des résultats, nous performons l'étude de manière indépendante avec deux modèles basés sur deux discrétisations des équations en eau peu profonde, développées dans (Ricchiuto , 2014) et (Nikolos et Delis, 2009). L'approche proposée permet d'obtenir la variance des sorties et leur sensibilité à chaque paramètre indépendant, ce qui permet de construire une hiérarchie de paramètres qui dépend des conditions d'écoulement .

Mots clés : Runup, propagation incertitudes, analyse de la variance, amplitude, friction, bathymetrie

1. Introduction

The reliability of the prediction of free surface hydrodynamics in realistic applications depends on the level of complexity used for the physical modeling, which might involve empirical coefficients that are usually chosen fit some experimental data, and so involve a certain degree of uncertainty. The same is often true for environmental conditions (wave amplitudes and distributions), for the topography, etc. The capability to take into account these uncertainties in the numerical simulation is of great importance, one hand to predict extreme events such as floods, Tsunami inundations, etc, and on the other to allow a better understanding of the underlying physics.

Several stochastic methods exist in literature, going from Monte Carlo and sampling-based methods to perturbation methods and generalized polynomial chaos methods (for a more detailed review see e.g. [12]). For the shallow water equations, uncertainty propagation has been studied by Ge and Cheung [5]. They used a spectral sampling scheme based on Galerkin projection, combined with a standard Godunov-type scheme to asses to propagation of uncertainties in wave heights and slope on the propagation and runup of long waves. The objective of the present paper is different. Our aim is to provide an extensive description of the runup/flooding process by not only investigating the propagation of uncertainties, but by using a decomposition of the variance allowing to provide additional understanding of each parameter's contribution to the flow dynamics. To this end, we use two independent models, both based on a discretization of the shallow water equations, and compare the spatial and temporal distributions of the statistics and of the sensitivities to variations of the incoming wave amplitudes, of the friction coefficient, and of the slope being flooded. The models used are given by the residual distribution code of [7,8], and by the finite volume code of [6,4]. These are used as ``probes'' in a non-intrusive polynomial-based stochastic method. In particular, the non-intrusive polynomial chaos techniques used is also the basis for the sensitivity analysis, based on an ANOVA decomposition, as described in detail in [3]. The test chosen is sufficiently simple to clearly infer the physical influence of each parameter.

The structure of the paper is the following. In section 2 we briefly recall the shallow water equations and describe the numerical schemes underlying the two codes used in the experiments. Section 3 is discusses the non-intrusive polynomial chaos method and the ANOVA technique. Finally, section 4 is devoted to the description of the numerical experiment and to the discussion of the results. The paper is ended by a summary and by a number of perspectives on the possible applications of the techniques proposed.

2. Numerical model: shallow water and related numerics

This paper is based on the modeling of free surface flows by means of the standard depth averaged shallow water equations which we write compactly as

$$\partial_t \begin{bmatrix} h \\ h\vec{v} \end{bmatrix} + \nabla \cdot \begin{bmatrix} h\vec{v} \\ h\vec{v}\otimes\vec{v} + gh^2/2\,\mathbf{I}_2 \end{bmatrix} = -gh \begin{bmatrix} 0 \\ \nabla b + \tau_f \end{bmatrix} \tag{1}$$

h being the water depth, $\vec{v}$ the depth averaged velocity, b the bathymetry, and g the gravity acceleration. The free surface level is denoted by $\eta = h + b$. The friction on the bathymetry level is modeled by

$$\tau_f = n^2 \frac{\|\vec{v}\|}{h^{4/3}} \vec{v} \tag{2}$$

with n the so-called Manning coefficient. The numerical experiments discussed later have been performed with two codes discretizing the shallow water system on unstructured triangular grids. The basics of the two method are briefly recalled in the following two sections.

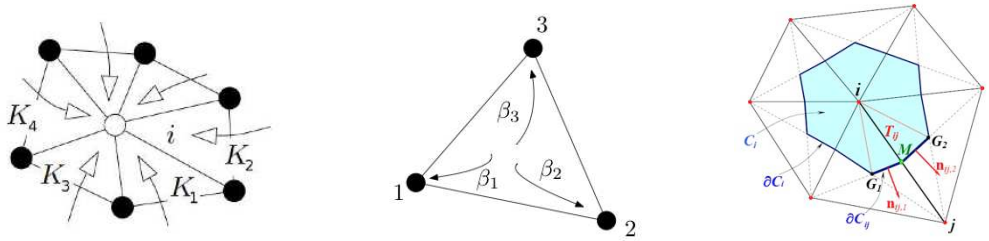

FIGURE 1 : Residual distribution method: assembly (left), distribution (middle), and median dual cell (right)

2.1 Cell-vertex residual distribution code

The first model is based on the explicit predictor corrector implementation of residual distribution discussed iin [7,8] (see also [9]). Setting $W = [h \;\; h\vec{v}]^t$, the scheme can be succinctly written as

$$|C_i|\frac{W_i^* - W^n}{\Delta t} = -\sum_{K\in K_i} \beta_i^K \phi^K(W^n)$$
$$|C_i|\frac{W_i^{n+1} - W_i^*}{\Delta t} = -\sum_{K\in K_i} \beta_i^K \Phi^K(W^*, W^n) \tag{3}$$

where $|C_i|$ is the area of the standard median dual cell obtained joining gravity edge mid-points with triangles gravity centers (cf. Figure 1 for the notation), K denotes the generic element of the mesh, the subscript i refers to the nodal value of the unknown, K_i denotes the set of elements sharing node i, the superscript * denotes the predicted value, the superscripts ^{n} and $^{n+1}$ refer to the old and new time levels, and Δt is the time step. Both the predicted and the corrected value of the unknown are expressed as a weighted average of elemental residuals, the weights (distribution coefficients) being denoted by β_i^K. The elemental residuals needed for the predictor are computed as

$$\phi^K(W) = \oint_{\partial K} \begin{bmatrix} h \\ h\vec{v} \end{bmatrix} v\cdot\hat{n}\, dl + \oint_{\partial K} \begin{bmatrix} 0 \\ gh^2/2 \end{bmatrix} \hat{n}\, dl + \int_K gh \begin{bmatrix} 0 \\ \nabla b + \tau_f \end{bmatrix} d\Omega \tag{4}$$

with all integrals evaluated using gauss quadrature and a linear continuous interpolation of the nodal values of the physical quantities. The corrector step, instead, uses complete element residuals computed as

$$\Phi^K(W^*, W^n) = \int_K \frac{W^* - W^n}{\Delta t} d\Omega + \frac{1}{2}\phi^K(W^*) + \frac{1}{2}\phi^K(W^n) \tag{5}$$

where again all integrals are evaluated using a continuous linear interpolation for the unknown over the triagle. The keys of the method are the definition of the quadrature used to evaluate the elemental residuals, and the definition of the distribution coefficients β_i^K. In particular, using a linear variation for both depth and bathymetry, the numerical quadrature is performed in a way that guarantees that if the free surface level η is constant (flat surface), and $\vec{v} = 0$, then one identically has $\phi^K = 0$. This allows to preserve indefinitely this lake at rest state (well balanced scheme). The definition of the distribution coefficients, on the other hand, is based on a nonlinear variant of a Lax-Friedrich's type scheme. For details concerning this and other aspects, including the treatment of moving shorelines, we refer the interested reader to [8,9].

2.2 Cell-vertex finite volume code

The finite volume code of [6,4] is based on a standard conservative approximation obtained by integrating (1) over the media dual cell C_i and applying Gauss theorem, leading to

$$|C_i|\frac{dW_i}{dt} = -\sum_{C_i\cap C_j\neq 0} \widehat{F}_{ij} - S_i \tag{6}$$

where, with reference to the notation of the rightmost picture in Figure 1, the term $\widehat{F}_{ij}$ is the finite volume numerical flux integrated along the boundary ∂C_{ij}, separating node i from node j, and projected along the direction of the normal to the boundary. The source term S_i is an approximation of the integral over the median dual cell C_i of the bathymetry and friction terms. In practice, we have used Roe's numerical flux evaluated using a classical MUSCL reconstruction with van Albada limiter. The source term, instead, is evaluated separating the contribution due to the variations of the bathymetry from those of the friction. For the bathymetry source, the well-balanced upwind bias originally introduced in [2] is used, together with an ad-hoc treatment of wet-dry interfaces allowing to preserve the lake at rest state also in presence of dry areas. The ordinary differential equation (6) is integrated with a semi-implicit procedure, using a second order four stages Runge-Kutta scheme with enhanced stability for the Roe fluxes and bathymetry source term, and with an implicit treatment of the friction. For details concerning this and other aspects, including the treatment of moving shorelines, we refer the interested reader to [6,4].

3. Uncertainty propagation and ANOVA

The discrete equations describing our free surface model are now used as a means of computing a certain output of engineering interest, depending on space, time, and on a set of physical parameters. So we look at the problem

$$\mathcal{L}(x,t,\xi;\, u(x,t,\xi)) = \mathcal{S}(x,t,\xi) \tag{8}$$

where u can be either one of the components of W computed from (3) or (6), or a functional depending on W, while the operator $\mathcal{L}$ and the forcing $\mathcal{S}$ are basically schemes (3) or (6) plus boundary and initial conditions. Randomness is introduced in (8) though the model parameters, boundary and initial conditions, though the vector of parameters ξ, which is assumed to have dimension (number of uncertain parameters) equal to d, and to be defined over a complete probability space, characterized by the space of the realizations, by a probability measure, and by an appropriate algebra (see [3] for details). The global Probability Density Function (PDF) $p(\xi)$ is defined as a joint probability from the independent PDFs of each parameter, in other words $p(\xi) = \Pi_{i=1,d}\, p_i(\xi_i)$. This assumption allows an independent polynomial representation for every direction in probabilistic space with the possibility to recover the multidimensional representation by tensorization. The aim of uncertainty quantification is to provide an improved representation of $u(x,t,\xi)$ given by the distribution in time and space of its statistical moments: average, variance, skewness, etc. In the following the dependence of u on space and time is dropped for simplicity.

3.1 Non-intrusive polynomial chaos

The technique used here to propagate the uncertainties is the non-intrusive Polynomial Chaos first introduced by Wiener [11], and used here in the form of the so-called generalized Polynomial Chaos [1] in which, for a given continuous probability distribution, the optimal set of polynomials is chosen as basis is chosen, such as for example the orthogonal basis of the Askey scheme [1]. Let Ψ_k denote the generic element of the basis, for $k=1,...,$P+1. The necessary number of functions in the polynomial expansion depends on the polynomial degree p, and on the number of parameters d as

$$\mathrm{P}+1 = \frac{(p+d)!}{p!d!} \tag{9}$$

In practice, the implementation of the method follows four steps

1. An efficient quadrature method (in d-dimensional parameter space) is selected to define ξ_j, $j=1,..,$N;
2. The codes (namely eq.s (3) or (6)) are used as probes to provide samples of the output u_j, $j=1,..,$N;
3. Use the samples to evaluate the integrals defining the coefficients of the polynomial expansion

$$\beta_k = \frac{\int\limits_{\Omega_\xi} u(\xi)\Psi_k(\xi)p(\xi)d\xi}{\int\limits_{\Omega_\xi} \Psi_k^2(\xi)p(\xi)d\xi} = \frac{\langle u(\xi),\Psi_k(\xi)\rangle_p}{\langle \Psi_k(\xi),\Psi_k(\xi)\rangle_p} \approx \frac{\sum\limits_{j=1}^{\mathrm{N}} w_j u_j \Psi_k(\xi_j)p(\xi_j)}{\langle \Psi_k(\xi),\Psi_k(\xi)\rangle_p} \tag{10}$$

4. Use the coefficients of the polynomial expansion to evaluate expected value $\overline{u}$, variance σ^2, etc:

$$\begin{aligned} \overline{u} &= \beta_0 \\ \sigma^2 &= \sum_{k=1}^{\mathrm{P}} \beta_k^2 \langle \Psi_k,\Psi_k\rangle_p \end{aligned} \tag{11}$$

For further discussion on possible quadrature approaches, as well as details concerning the convergence of the method w.r.t. the number of samples and polynomial degree, we refer to [3].

3.2 ANOVA decomposition and sensitivity indexes

The sensitivity analysis comes out somewhat for free from the non-intrusive polynomial chaos method, as extensively discussed in [3]. The underlying assumption of the analysis is the existence of the so-called Sobol decomposition reading

$$u(\xi) = \overline{u} + \sum_k u_k(\xi_k) + \sum_{l<k} u_{kl}(\xi_k,\xi_l) + ... + u_{1...d}(\xi_1,...,\xi_d) = \overline{u} + \sum_{s=1}^{d} \sum_{i_1<...<i_s} u_{i_1...i_s}(\xi_{i_1},...,\xi_{i_s}) \tag{12}$$

The main interest of the decomposition is that each one of the terms represents the dependence of the output on a selected number of parameters. With the exception of the first term, given by the average expectation, all terms have a null first order moment, while they do contribute to the variance. In particular, one can easily prove that, due to the assumed independence of the terms involved, the total variance is given by the sum of all the conditional contributions of each term, namely

$$\sigma^2 = \sum_{s=1}^{d} \sum_{i_1<\ldots<i_s} \sigma^2_{i_1\ldots i_s} \tag{13}$$

The Sobol sensitivity and total sensitivity indexes are then defined as

$$\mathrm{S}_{i_1\ldots i_s} = \frac{\sigma^2_{i_1\ldots i_s}}{\sigma^2}, \quad \mathrm{TSI}_j = \sum_{s=1}^{d} \sum_{j\in\{i_1,\ldots,i_s\}} \mathrm{S}_{i_1\ldots i_s} \tag{14}$$

and represent respectively the contributions to the variance of the output u of each independent parameter/group of parameters, and the total contribution of a single parameter (including coupled effects). In practice, it is shown in [3] that the set of indices $\{i_1,\ldots,i_s\}$ allows to uniquely define a subset of the tensorial basis $\{k_{i1},\ldots,k_{is}\}$ used for the gPC expansion which are representative of only the subset of parameters associated to the set of indices $\{i_1,\ldots,i_s\}$. This allows to immediately compute the conditional contributions as (cf. equation (11))

$$\sigma^2_{i_1,\ldots,i_s} = \sum_{k\in\{k_{i1},\ldots,k_{is}\}} \beta_k^2 \langle \Psi_k, \Psi_k \rangle_p \tag{15}$$

allowing immediately to obtain the sensitivity indexes from the non-intrusive polynomial chaos method. We refer the interested reader to [3,10] for further details.

4. Numerical experiment: runup on a constant slope

The numerical experiment performed is that of a solitary wave runup over a slope. The test has been chosen not only to asses the computational procedure, but to investigate the physics of the runup process and the sensitivity to the different parameters in a sufficiently simple framework.

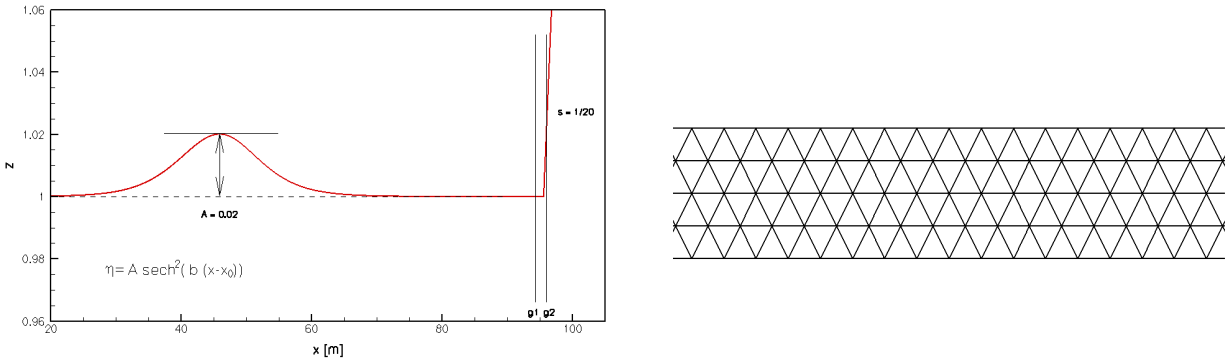

FIGURE 2 : Numerical experiment: solitary wave runup. Left: sketch of the initial solution with superimposed the position of the gauges. Right: topology of the computational grid used for the simulations.

The initial solution, sketched on the left on Figure 2, consists of a solitary wave with a profile given by the classical squared hyperbolic secant. The slope of the bathymetry over which the runup takes place is 1/20. Uncertainties are assumed for the amplitude of the wave, for the slope of the bathymetry, and for the friction coefficient n (cf. equations (1) and (2)). These parameters are assumed to have a uniform PDF with a variation of 10% around the average value of 2cm for the amplitude, and of 5% around the average value of 1/20 for the slope. The friction coefficient is instead assume to vary uniformly in the range 0.005-0.05. The simulations have been run on two-dimensional meshes with the topology shown on the right on Figure 2. The results which we look at are he free surface distribution in space at times t=20s and t=30s, roughly corresponding to the beginning of the runup process and to the finishing phase of the backwash, and the time evolution of the free surface level in two gauges placed at the position of the maximum 'wet' free surface and at the wet/dry interface at time t=20s (in the deterministic computations).

4.1 Deterministic and stochastic results

We start by comparing the spatial evolution obtained with deterministic computations, run with average values of the parameters, with those of the stochastic simulations presented in terms of expected mean value and mean plus/minus twice the deviation. The results are summarized on Figure 3. Several remarks can be made. First of all, the results obtained with the two codes are barely distinguishable. We have repeated the test on several meshes with spacings from 40cm to 5cm (the

length of the channel is 100m), and we had to look very close to see any substantial differences between the two models. Concerning the differences between the deterministic and the stochastic results, we can clearly see that the runup phase (top pictures) shows a relatively small deviation in the wet region (roughly on the left of the second gauge), and a larger one in the dry part, which is basically mainly due to the uncertainty on the slope. Conversely, during backwash we find a much larger deviation within the wet region (in between the gauges and on the left of the first gauge). This gives important information on the runup process: the most critical phase, as far as parameter dependence is concerned, is the backwash.

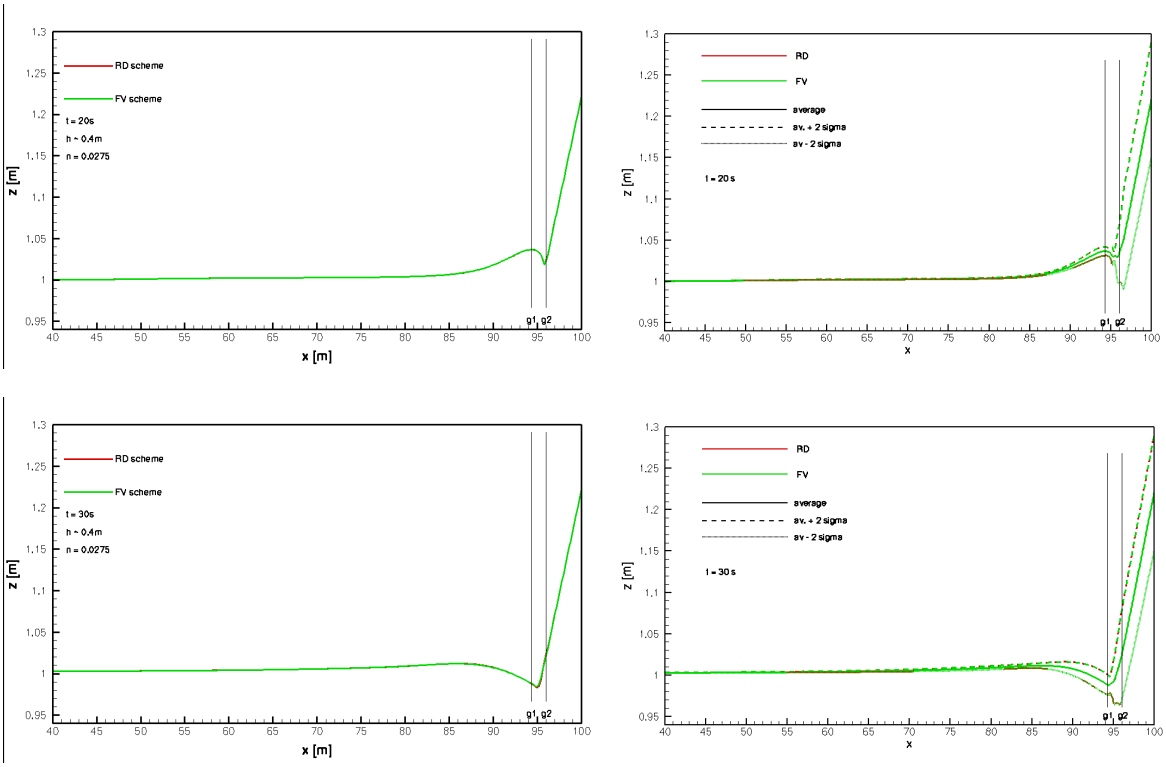

FIGURE 3 : Free surface level at times t=20s (top) and t=30s (bottom). Deterministic results obtained using average values of the parameters (left), and expected mean plus minus twice the deviation (right).

We then look at the temporal evolution of the free surface in gauges. The deterministic computations are shown on the top picture on Figure 4. Again both models give identical results. In gauge g1 we see the water level increasing due to the runup process, and then decrease below the initial stationary value during backwash, and go back up for a secondary runup phase. Gauge g2 is instead more interesting. We see the water level remaining constant before the arrival of the water front. Then we can clearly follow the runup phase, during which the amount of water increases, and the backwash phase with a trailing tail, leading back to the initial value of water height, which is certainly due to the effects of friction. The stochastic results are reported on the bottom of the same figure. As for the spatial evolution, we observe a clear difference in the behavior in g1, with a relatively tighter deviation, which is maximal at the beginnig of the runup (time t~20s) and toward the final phase of the backwash (t~28s). The gauge g2 shows instead a large variation during all times, due to a large sensitivity to slope variations, but also during the 'wet' phase, and especially toward the end of backwash, confirming once more the sensitivity of this phase to variations in the parameters.

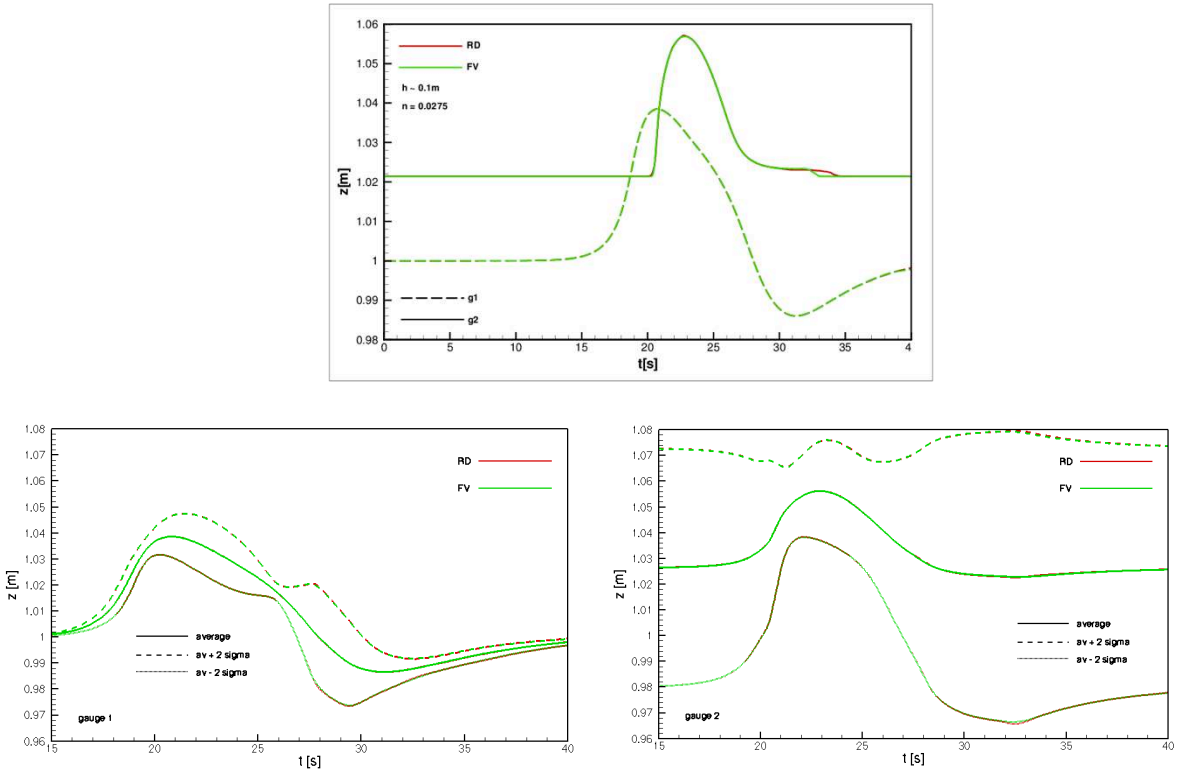

FIGURE 4 : Time evolution of the free surface in the gauges. Top: deterministic results. Bottom: stochastic results (mean plus/minus twice the deviation) in gauge 1 (left) and gauge 2 (right)

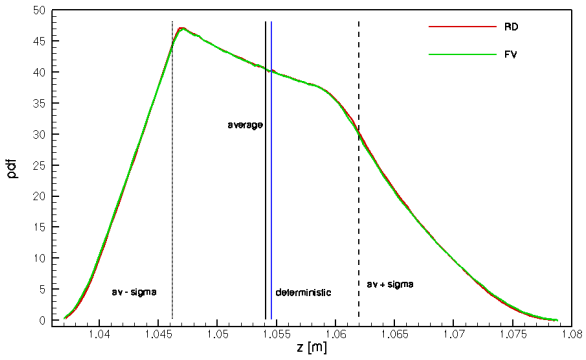

FIGURE 5 : Probability density function of the value of water height in gauge g2 at time t=25s (approximately the time of maximum depth in the deterministic computations).

Before looking at the parameter sensitivities, we report on Figure 5 the numerically reconstructed probability density function ot the value of water height in gauge g2 at time t=25s, which roughly corresponds to the time of maximum depth in the deterministic results. The first important remark is that, even with a uniform variation of the parameters, the PDF is highly irregular, and presents a large skewness with a sharper head and a longer tail. The average and deterministic values, reported in the figure, are quite close.

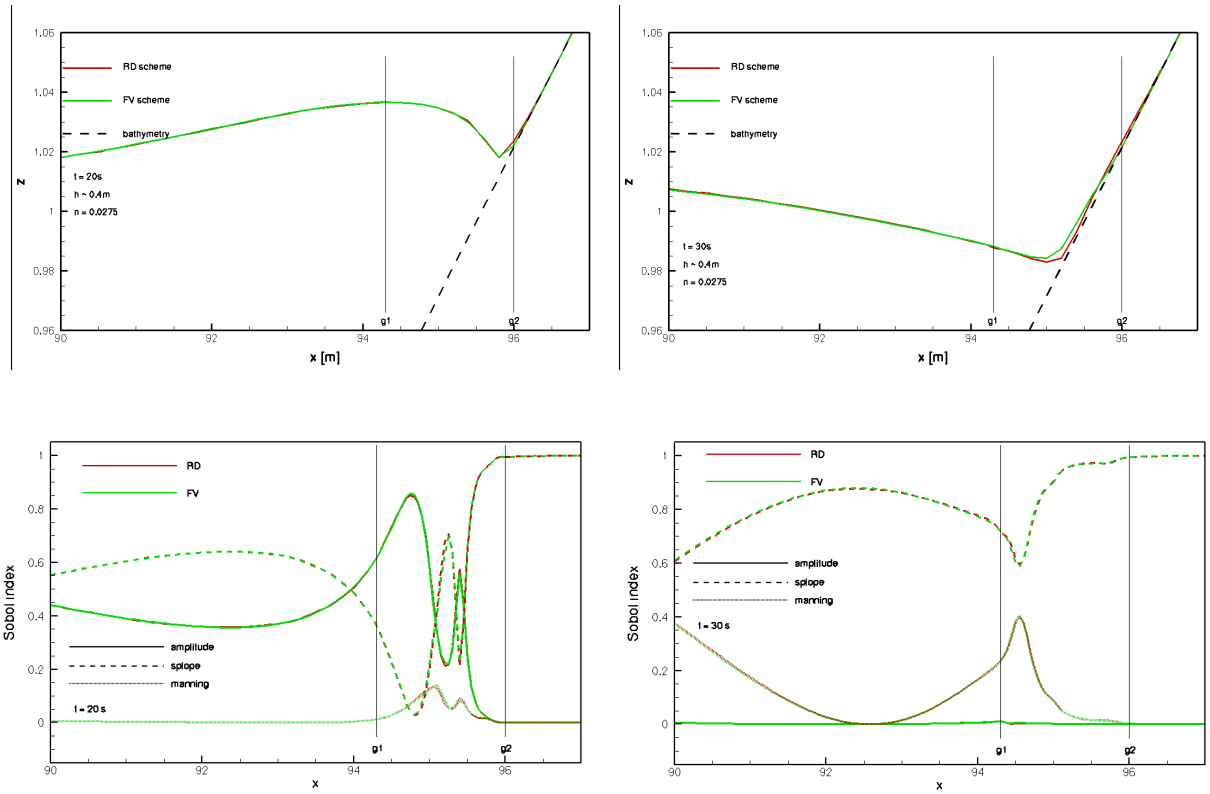

FIGURE 6 : Sensitivity analysis for amplitude, Manning coefficient and slope at times t=20s (left) and t=30s (right). Top: deterministic free surface levels, bottom Sobol sensitivity indexes.

4.2 Parameter sensitivity analysis

Finally, we look at the spatial and temporal distributions of the sensitivity indexes. As done before, we start with their distribution in space at times t=20s and t=30s. The results are summarized on Figure 6 where, for completeness, we report a close up of the deterministic free surface distribution. The results at time t=20s (left pictures) show that amplitude and bathymetry slope are the dominating parameters with a significantly smaller contribution of the friction (below 10%). Conversely, at time t=30s (right pictures) the amplitude plays virtually no role, the dynamics of the backwash being dominated by the friction and by the slope. Considering that the backwash has been seen to be the most sensitive phase of the process, this shows the enormous impact of the definition and modeling of friction.

Lastly, we report on Figure 7 the temporal evolution of the sensitivity indexes in gauges g1 and g2. For completeness, the pictures showing the stochastic evolution of the free surface are reported in the same figure. The behavior observed in g1 (left pictures) confirms all the previous observations: amplitude and slope dominate the initial phase of the runup; friction becomes a major player during backwash. The results in g2 are unfortunately hard to interpret, the bathymetry being clearly the dominating factor in the variations observed, amplitude and Manning coefficient giving quantitatively very close contributions.

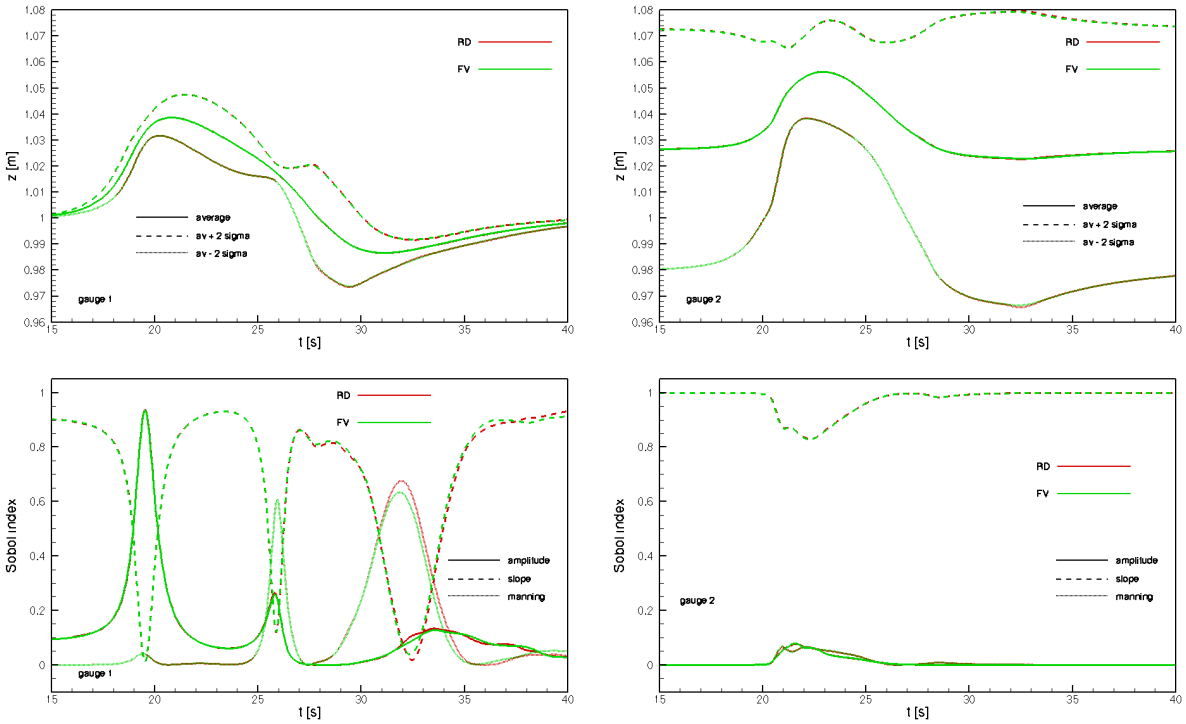

FIGURE 7 : Sensitivity analysis for amplitude, Manning coefficient and slope at gauge g1 (left) and g2 (right). Top: stochastic history of free surface level, bottom Sobol sensitivity indexes.

Conclusion and perspectives

In this paper we have discussed a parametric study of the runup process using uncertainty quantification tools and ANOVA decomposition for parameter sensitivity analysis. The study has been conducted with two independent models to ensure that the behaviors observed are independent on the numerics as much as possible. The results have shown that indeed a hierarchy of parameters exists during the flooding process but also that this hierarchy is not constant neither through time nor space. In particular, we have see that for a simple runup test, flooding heights mainly depend on slope and incoming wave amplitude. However, the backwash dynamics show dominant effects of the friction, which means that in more complex situations involving wave reflections and interactions the two effects might interact. Besides the inherent physical interest, the study has allowed an extended comparison and benchmarking of the two models which we believe should become a standard procedure.

Future developments will involve of course the study of more complex scenarios involving both dam break and Tsunami runup on complex bathymetries. An interesting development would be the comparison of more complex models, such as Boussinesq equations, and the study of the influence of epistemic uncertainty, namely the uncertainty due to the choice of the model (form of friction term, dispersive model opposed to shallow water, etc.)

Acknowledgements

M. Ricchiuto and P. Congedo are partially funded by the project PIA-RSNR TANDEM.

Bibliography

[1] Askey, R. and Wilson, J. (1985). Some basic hypergeometric polynomials that generalize Jacobi polynomials, *Memoirs Amer.Math. Soc.*, **319**.

[2] Bermudez, A. and Vazquez, E. (1993). Upwind methods for hyperbolic conservation laws with source terms, *Computers and Fluids*, **23**, 1049-1071.

[3] Crestaux, T., LeMaitre O. and Martinez, J.-M. (2009). Polynomial chaos expansion for sensitivity analysis, *Reliability Engineering and System Safety* **94**,1161-1172.

[4] Delis, A.I., Nikolos I.K. and Kazolea, M. (2011). Performance and comparison of cell-centered and node-centered unstructured finite volume discretizations for shallow water free surface flows, *Archives of Computational Methods in Engineering*, 18, 1-62.

[5] Ge, L. and Cheung, K. (2011). Spectral Sampling Method for Uncertainty Propagation in Long-Wave Runup Modeling, *Journal of Hydraulic Engineering*, **137**, 277-288.

[6] Nikolos, I.K. and Delis, A.I. (2009). An unstructured node-centered finite volume scheme for shallow water flows with wet/dry fronts over complex topography, *Computer Methods in Applied Mechanics and Engineering*, **198**, 3723-3750.

[7] Ricchiuto, M. and Bollermann, B. (2009), Stabilized residual distribution for shallow water simulations, *J.Comput.Phys,* **228**, 1071-1115.

[8] Ricchiuto, M. (2011), Explicit Residual discretizations for shallow water flows, *AIP Conf. Proc.,* **1389**(1), 919-922.

[9] Ricchiuto, M. (2014), An explicit well balanced residual based approach to free surface flow simulation, INRIA Report RR-8350, in revision on *J.Comput. Phys.*

[10] Sobol, I.M. (2001). Global sensitivity indices for nonlinear mathematical models and their Monte Carlo estimates, *Mathematics and Computers in Simulation*, **55**, 271-280.

[11] Wienxer, N. (1938). The Homogeneous Chaos, *American Journal of Mathematics*, **60**, 897-936.

[12] Xiu, D., (2009). Fast numerical methods for stochastic computations: a review, *Communications in Computational Physics*, **5**, 242-272.

RESEARCH CENTRE
BORDEAUX - SUD-OUEST

351 Cours de la Libération
Bâtiment A29
33405 Talence Cedex France

Publisher
Inria
Domaine de Voluceau - Rocquencourt
BP 105 - 78153 Le Chesnay Cedex
inria.fr
ISSN 0249-6399